Comparison of microrings and microdisks for high-speed optical modulation in silicon photonics

Zhoufeng Ying, Zheng Wang, Zheng Zhao, Shounak Dhar, David Z. Pan, Richard Soref, and Ray T. Chen

Citation: Appl. Phys. Lett. **112**, 111108 (2018); doi: 10.1063/1.5019590
View online: https://doi.org/10.1063/1.5019590
View Table of Contents: http://aip.scitation.org/toc/apl/112/11
Published by the American Institute of Physics

Comparison of microrings and microdisks for high-speed optical modulation in silicon photonics

Zhoufeng Ying,[1] Zheng Wang,[1,2] Zheng Zhao,[1] Shounak Dhar,[1] David Z. Pan,[1] Richard Soref,[3] and Ray T. Chen[1,2,4,a)]
[1]*Department of Electrical and Computer Engineering, The University of Texas at Austin, Austin, Texas 78712, USA*
[2]*Materials Science and Engineering Program, Texas Materials Institute, The University of Texas at Austin, Austin, Texas 78712, USA*
[3]*Department of Engineering, University of Massachusetts Boston, Boston, Massachusetts 02125, USA*
[4]*Omega Optics, Inc., 8500 Shoal Creek Blvd., Bldg. 4, Suite 200, Austin, Texas 78757, USA*

(Received 14 December 2017; accepted 6 March 2018; published online 15 March 2018)

The past several decades have witnessed the gradual transition from electrical to optical interconnects, ranging from long-haul telecommunication to chip-to-chip interconnects. As one type of key component in integrated optical interconnect and high-performance computing, optical modulators have been well developed these past few years, including ultrahigh-speed microring and microdisk modulators. In this paper, a comparison between microring and microdisk modulators is well analyzed in terms of dimensions, static and dynamic power consumption, and fabrication tolerance. The results show that microdisks have advantages over microrings in these aspects, which gives instructions to the chip design of high-density integrated systems for optical interconnects and optical computing. *Published by AIP Publishing*. https://doi.org/10.1063/1.5019590

The limitations of electrical interconnects in terms of speed and power consumption are becoming more and more obvious as the transistors continue to shrink in size. This has led to the emergence of optical interconnects, penetrating from long-haul communication to on-chip communication and even to intra-chip interconnects.[1,2] In integrated interconnects, silicon photonics has been picked up by the industry to be one of the leading candidates due to its unique properties of low latency, low dissipation, and high bandwidth, as well as its compatibility with the most mature manufacturing line, complementary metal–oxide–semiconductor (CMOS), leading to low fabrication costs.[3–6]

As one type of key component in optical interconnects, optical modulators have been well investigated recently and various ultrahigh-speed compact modulators have been demonstrated.[7] Among them, Mach-Zehnder interferometer (MZI) based modulators always exhibit a large footprint (few hundreds of microns to millimeters) and consume a considerable amount of power due to large driving voltages and high capacitance.[8,9] Electro-absorption modulators, for example, germanium-on-silicon modulators, exploiting the strong Franz-Keldysh and quantum-confined Stark effects, also require relatively large power due to the additional power transition from light to photocurrent. Further, it normally operates in a modest wavelength range because of the band-edge effect, which can be engineered but at the cost of higher fabrication complexity.[10] Alternately, resonant structures that confine light in a small volume are able to efficiently enhance the interaction between light and a waveguide with a subtle refractive index change, leading to high-speed and low-power modulators as well as enabling wavelength division multiplexing (WDM) to scale bandwidth.[11–13] The first electro-optical silicon ring modulator was demonstrated by Xu *et al*. in 2005, which exploits the carrier injection in a p-i-n junction.[14] However, the modulation bandwidth of this injection-based structure (~few Gb s^{-1}) is limited by the free-carrier lifetime in silicon diodes and a complex pre-emphasis driving signal is required to achieve higher-speed operation with increased power consumption and CMOS complexity.[15] Instead, carrier depletion-based modulators were proposed to overcome these limitations. For instance, a 56 Gb s^{-1} depletion-based ring modulator was demonstrated in 300 mm CMOS platform with record performances of 4 dB dynamic extinction ratio and 45 fJ/bit dynamic power consumption using 2.5 Vpp drive swing.[16] On the other hand, another resonant structure, i.e., microdisk, is also well investigated especially with the development of vertical junctions. A demonstration of a high-speed (25 Gb s^{-1}) and efficient (0.9 fJ/bit) disk modulator was implemented by Timurdogan *et al*. in 2014.[13] Because of these excellent performances of microresonator based modulators as well as the urgent requirement of low power consumption, high bandwidth, and high integration, more and more researchers are now using this kind of modulator as the key modules in their applications and products and it will continue to bloom in the future single-digit femtojoule-class communications in datacenters and supercomputers. Therefore, their characteristics should be investigated and compared thoroughly, which will contribute to the selection of fundamental modules in designing power-efficient and high-speed communication or computing architectures in the future.[6,17–20]

In this paper, the performances of microrings and microdisks are comprehensively compared in terms of dimensions, power consumption, and fabrication tolerance. The theoretical and experimental results show that the microdisks will be a preferred option in a low-power-consumption and high-density integrated system since it occupies less on-chip space, tolerates more critical dimension (CD) variation, and consumes less power including dynamic and static power.

a)Electronic mail: chenrt@austin.utexas.edu

Figure 1 depicts our fabricated microdisk and microring structure on a silicon-on-insulator (SOI) substrate as well as the mode profiles from two views. As can be seen from Figs. 1(b) and 1(c) and 1(e) and 1(f), these two structures exploit two different mechanisms to confine and guide light despite the similarity in shape. Microrings utilize the bending waveguide mode with two physical side-walls confining the light while the microdisks use the whispering gallery mode which only relies on one curved boundary. This intrinsic difference eventually leads to many subsequent differences in performance.

The device footprint is an obvious and yet significant feature that needs to be considered in the first place. Compared to microrings that need to leave ridges near the core waveguide for junction doping and electrode contacts, microdisks allow both p and n contacts to be made totally inside the disk and etch through the Si layer outside the boundary. As a result, it forms a hard wall for better optical confinement and eventually enables even smaller disk size that potentially reduces the capacitance and power consumption as well as offers a large free spectrum range (FSR) for more efficient WMD or even dense WDM (DWDM). For example, as the principal figure of merit of a resonator, the internal quality factor of a microdisk resonator with a radius of 1.5 μm is comparable to that of a microring resonator with a radius of 4.5 μm.[13] In practice, either in academia or in industry, most of the ring modulators that have been demonstrated so far are around 10 μm in diameter[14–16] while disk modulators could achieve smaller than 5 μm in diameter,[13,21] also as shown in Figs. 1(a) and 1(d), which leads to larger than 4 times improvement in on-chip space saving, beneficial for high-density optical integration with an advanced CMOS integrated circuit. It should be noted that a high Q-factor is not always desired especially for a high-speed modulator since the optical frequency response is governed by the photon lifetime. The fastest microdisk modulator to date is 44 Gb s^{-1} with a Q-factor of ~6000,[13] and the microring modulator is 56 Gb^{-1} with a Q-factor of 3500.[16] Increasing the doping will reduce the Q-factor and therefore increase the bandwidth, at the expense of higher insertion loss and less extinction ratio.

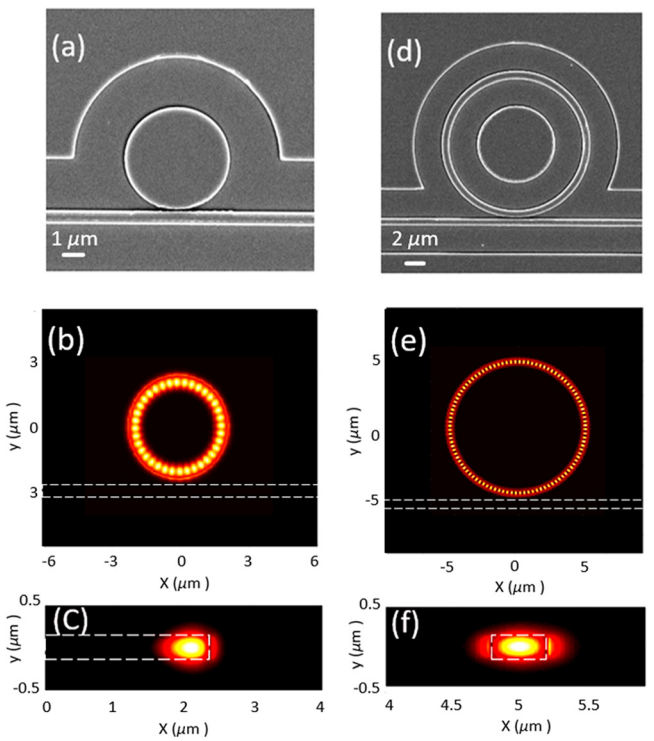

FIG. 1. (a)–(c) show the SEM picture of a microdisk with a radius of 2.4 μm as well as the mode profiles of top view and cross section. (d)–(f) depict the case for a microring with a radius of 5 μm.

Resonant structures inevitably suffer from their high sensitivity to CD variation. Specifically, a deviation of 1 nm in the width of the ring waveguide can result in 0.25 nm shift in the resonant wavelength.[22] However, the quality factors of traditional microresonators are always lying in the range of several thousands to several tens of thousands, which means that the 3 dB bandwidths would be smaller than 1 nm if the operating wavelength locates at the C-band. Thus, several nanometer deviation in fabrication is already large enough to significantly affect the whole system and even totally put the device in an inoperable state. Considering this almost ineradicable fabrication tolerance, in practice, people usually choose to utilize heaters to set the wavelength to a desired one or align multiple wavelengths to one peak at a cascaded resonator system. Obviously, the CD variation range directly determines the power amount that is required to align the wavelength.

Therefore, we investigate the sensitivity of the wavelength shift with respect to CD variation of both structures in the simulation and experiment. In the real fabrication process, especially in the silicon etching step, the CD variation will mostly affect the width of the ring and the radius of the disk, respectively, since the ring has two sides that can be affected simultaneously while the disk has only one side exposed, as shown in Fig. 2(a). The rings and disks deviate an equivalent amount at each side in the same nanofabrication procedure. Given that $n_r L = m\lambda_r$ for the mth-order resonance in a resonator with the length of L, one can obtain $\Delta\lambda_r/\Delta n_r = L/m = \lambda_r/n_r$. Therefore, in theory, the wavelength shift for a ring can be calculated as

$$\Delta\lambda_r = \frac{\Delta\lambda_r}{\Delta n_r} \cdot \frac{\Delta n_r}{\Delta w_r} \cdot \Delta w_r = \frac{k\lambda_r \Delta w_r}{n_r}, \tag{1}$$

where $k = \Delta n_r/\Delta w_r$ means the sensitivity of the group refractive index of the guided mode versus the width deviation w_r, λ_r is the resonant wavelength, n_r is the group refractive index of the guided mode, w_r is the width of the microring waveguide, and the prefix Δ is the deviation of the corresponding parameters. Similarly, the wavelength shift for a disk is given by

$$\Delta\lambda_d = \frac{\lambda_d \Delta r_d}{r_d}, \tag{2}$$

where λ_d is the resonant wavelength, r_d the radius, and Δr_d the deviation of the radius. As an estimate, we set $\lambda_r = \lambda_d = 1.55\,\mu$m, $r_d = 2.4\,\mu$m, and $r_r = 5\,\mu$m along with $\Delta w_r = 2\Delta r_d$. Then, using simulation software, one could easily obtain $n_r = 4.5$ and $k = 5.5\,\mu m^{-1}$. Therefore, the sensitivity ratio of microrings and microdisks could be calculated as $\Delta\lambda_r/\Delta\lambda_d = 5.9$, which means that the resonant wavelength

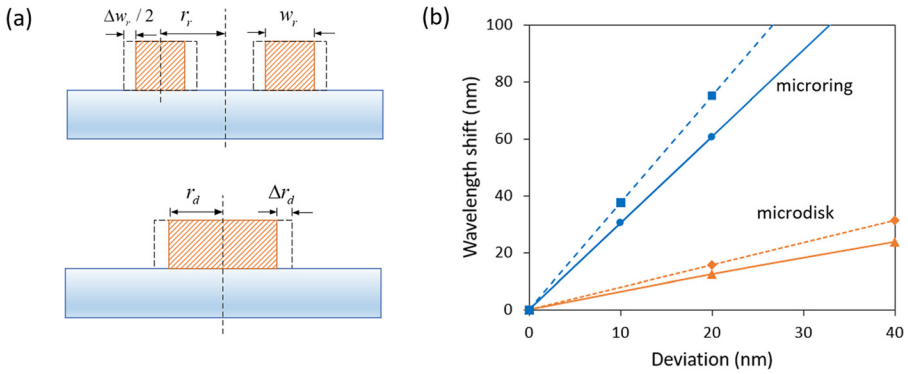

FIG. 2. (a) The different dimensional change to a microring and a microdisk resulting from CD variation. (b) The simulation (dotted lines) and experimental (solid lines) results of the wavelength shift of microrings and microdisks with respect to the CD variation.

of microrings will shift around six times more than microdisks as a response to the same deviation. Various microrings and microdisks with designated width/radius variations are then simulated and fabricated to demonstrate the theoretical conclusion. All the simulations in this paper were performed with commercial software Lumerical Mode. Devices were fabricated on p-type silicon-on-insulator wafers from SOITEC with a 3 μm buried oxide layer and a thin top silicon layer of 220 nm. The waveguides were defined by E-beam lithography and formed by reactive ion etching. The waveguide is 450 nm in width and 220 nm in height. A large dynamic range of deviations is chosen here for two purposes. First, it can eliminate the influence of unpredictable real CD errors which is more than one order of magnitude smaller. Second, it meets the fabrication resolution. The testing results are shown in Fig. 2(b) with the axis denoted as Δr_d, i.e., the deviation of a disk, which is also a half of Δw_r. It can be obtained easily from the figure that the ratios of the wavelength shift of the microrings and microdisks to the deviation are ~3 and 0.5, respectively, which indicates that, compared to microrings, microdisks are six times less sensitive to the fabrication deviation, agreeing well with our expectation mentioned above. Further, in order to observe the real wavelength distribution and statistic performance, we fabricate eleven groups of identical microrings and microdisks in the same chip as shown in Fig. 3(a), which were placed alternately to reduce the potential influence of other factors such as the thickness variation of the SOI chip. The tested results are shown in Fig. 3(b). Multiple wavelengths peaks, R1, R2, R3, and R4, appear in the range with the FSR of 18.3 nm for microrings while only one D1 exists for microdisks due to different resonator dimensions. Figure 3(c) is a zoom-in figure of the distribution of R3 and D1 with eleven pairs of data dots. The distribution ranges of rings and disks are 3 and 0.8 along with the calculated variances of 1.1 and 0.09, consistent with the conclusion mentioned above. Note that the variation of the wavelength is much smaller than the FSR so that the smaller FSR of the microring modulator will not contribute to the active wavelength alignment which will be discussed hereinafter. The important implication is that the power consumption needed to adjust the resonant wavelengths of microdisks requires less power when compared with the microrings.

In order to tune the wavelengths to a desired position or align multiple wavelengths due to the fabrication error, metallic heaters are always fabricated on top of the microresonators to adjust the system parameters with the thermal-optical (TO) effect. Therefore, thermal sensitivity, which determines the power consumed to tune wavelengths, must be taken into consideration as another important factor for optical modulation. Given that the TO coefficient of silicon is $\alpha = 1.8 \times 10^{-4}\,\mathrm{K}^{-1}$,[23] the temperature-induced wavelength shift can be expressed as

$$\frac{\Delta\lambda}{\Delta T} = \frac{\alpha\lambda}{n}, \tag{3}$$

where n is the group index. $n_r \approx 4.5$ and $n_d \approx 3.7$ are chosen for an estimate based on the simulation results. Thus, the TO coefficient $\Delta\lambda/\Delta T$ for microrings and microdisks would be 62 pmK^{-1} and 75 pmK^{-1}. In other words, microdisks have 20% higher TO coefficient than microrings.

In the experiment, the whole chip was heated up from 35 °C to 65 °C using a thermoelectric-cooler (TEC)[24] and the temperature was measured using a thermodetector. The resonant peaks were recorded accordingly. From Fig. 4(a), the thermal sensitivity of the ring and the disk can be readily calculated as 0.08 nm/°C and 0.1 nm/°C with the ratio of 125%, which means that the microdisk is more temperature-sensitive and thus more easily to be tuned. Further, in order to accurately distinguish these microresonators from the

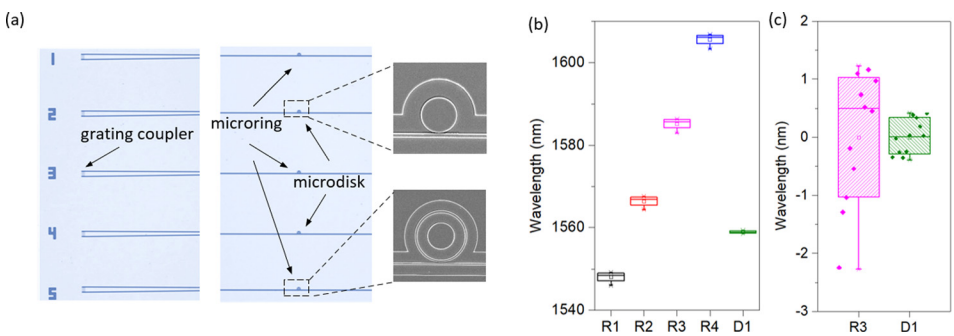

FIG. 3. (a) A micrograph of the fabricated arrays of microrings and microdisks. (b) The wavelength distribution of a group of identical microrings and microdisks. R1, R2, R3, and R4 represent the four adjacent resonant wavelengths of microrings, and D1 represents one wavelength of microdisks. (c) A zoom-in figure illustrates the different distribution for these two resonators.

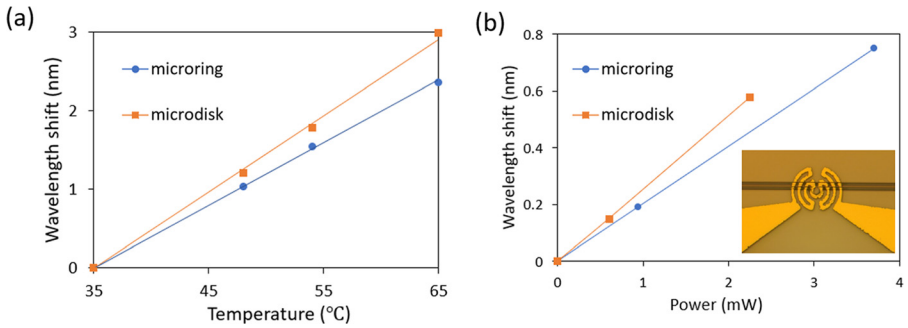

FIG. 4. Experiment results of the (a) temperature and (b) applied power induced wavelength shift. The inset shows the micrograph of a gold heater.

perspective of power consumption in a real device rather than the TO coefficient, identical microheaters with the thickness of 140 nm, shown in the insets in Fig. 4(b), were fabricated on the top of silicon structures with a 1.5 μm-thick SiO_2 layer as a separation.[25–27] The power-related wavelength shifts, as can be seen from Fig. 4(b), are 0.258 nm/mW for disks and 0.203 nm/mW for rings, respectively, with a ratio of 127%. Obviously, this result matches up with the theoretical and experimental TO coefficient. It also manifests that the power consumption for tuning is proportional to the temperature change. Moreover, the smaller footprint of microdisks will further contribute to saving power to align resonant wavelengths.

Besides the static power consumption, dynamic power consumption, defined as the power required to switch the states (ON/OFF) of the modulator, is another significant factor in an EO modulator that needs to be taken into consideration. The average dynamic power consumption is always estimated as $CV^2/4$ using the junction capacitance C and swing voltage V. Therefore, reducing the capacitance is important to achieve a power efficient modulator and obviously a reduced voltage is even more important since it emerges as a squared term. A small voltage is also preferred in the integration with advanced CMOS driving circuits, enabling the chip-scale electronic-photonic system.[6] As has been discussed above, the compactness of microdisks contributes to ultrasmall capacitance and larger overlap of the active region with the optical mode especially with the help of the vertical junction technique. As a result, less power would be needed for a microdisk to achieve an on/off switch, i.e., the dynamic power consumption. For example, a record microdisk modulator was presented in 2014 by Timurdogan *et al.* with the speed of 25 Gb s^{-1}, the swing voltage of 0.5 V, the capacitance of 17 fF, and the power consumption of <1 fJ/bit,[13] regarded as an important step towards realizing femtojoule per bit class communication links. As a comparison, Dong *et al.* demonstrated a racetrack based modulator with the swing voltage of 1 V, the capacitance of 40 fF, and the dynamic power consumption of 10 fJ/bit, operating at 12.5 Gb s^{-1}.[28] Another high-speed microring modulator functioning at 56 Gb s^{-1} with the capacitance of 30 fF, the swing voltage of 2.5 V, and the dynamic power consumption of 45 fJ/bit is also demonstrated recently.[16]

As the integrated silicon photonics develops especially after the involvement of industry, there is a trend that more and more people try to tape out their chips to foundries for fabrication and demonstration of photonic devices and systems, similar to the case for traditional VLSI. Therefore, whether a component is available in their libraries is a key fact that researchers should consider; otherwise, one has to design, fabricate, and test for numerous runs by himself which is very expensive and time-consuming. The performance could not be guaranteed as well. Fortunately, the two devices discussed above could be obtained successfully from foundries such as IMEC and AIM photonics. The fabrication processes of these two devices in foundries are very similar and actually researchers could focus more on performance and system integration rather than the fabrication details when cooperating with foundries.

In conclusion, we have compared both in the simulation and in the experiment the microrings and microdisks for high-speed optical modulation in integrated silicon photonics in terms of various modulation performances, including the footprint, fabrication tolerance, thermal tuning efficiency, and static and dynamic power consumption. The results show that a microdisk based modulator with a smaller footprint has less sensitivity to fabrication deviation, larger thermal tuning efficiency, and less dynamic power consumption, which provides instructions for the future chip design of a high-density integrated system.

The authors acknowledge support from the Multidisciplinary University Research Initiative (MURI) program through the Air Force Office of Scientific Research (AFOSR) (Grant No. FA 9550-17-1-0071), monitored by Dr. Gernot S. Pomrenke. R.S. acknowledges support from AFOSR on Grant No. FA9550-17-1-0354.

[1]C. Kachris and I. Tomkos, "A survey on optical interconnects for data centers," IEEE Commun. Surv. Tutorials **14**, 1021 (2012).
[2]D. Miller, "Optical interconnects to electronic chips," Appl. Opt. **49**, F59 (2010).
[3]R. Soref, "The past, present, and future of silicon photonics," IEEE J. Sel. Top. Quantum Electron. **12**, 1678 (2006).
[4]D. A. B. Miller, "Device requirements for optical interconnects to silicon chips," Proc. IEEE **97**, 1166 (2009).
[5]H. Subbaraman, X. Xu, A. Hosseini, X. Zhang, Y. Zhang, D. Kwong, and R. T. Chen, "Recent advances in silicon-based passive and active optical interconnects," Opt. Express **23**, 2487 (2015).
[6]C. Sun, M. T. Wade, Y. Lee, J. S. Orcutt, L. Alloatti, M. S. Georgas, A. S. Waterman, J. M. Shainline, R. R. Avizienis, S. Lin *et al.*, "Single-chip microprocessor that communicates directly using light," Nature **528**, 534 (2015).
[7]G. T. Reed, G. Mashanovich, F. Y. Gardes, and D. J. Thomson, "Silicon optical modulators," Nat. Photonics **4**, 518 (2010).
[8]M. Streshinsky, R. Ding, A. Novack, Y. Liu, X. Tu, A. E. J. Lim, E. K. Sing Chen, P. G. Q. Lo, T. Baehr-Jones, and M. Hochberg, "50 Gb/s silicon traveling wave Mach-Zehnder modulator near 1300 nm," in *Conference on Optical Fiber Communications Technical Digest* (2014), Vol. 21, p. 30350.
[9]X. Xiao, H. Xu, X. Li, Z. Li, T. Chu, J. Yu, and Y. Yu, "60 Gbit/s silicon modulators with enhanced electro-optical efficiency," in *Optical Fiber*

Communication Conference Fiber Optic Engineers Conference (2013), pp. OW4J.3.
[10]S. A. Srinivasan, M. Pantouvaki, S. Gupta, H. T. Chen, P. Verheyen, G. Lepage, G. Roelkens, K. Saraswat, D. Van Thourhout, P. Absil *et al.*, "56 Gb/s germanium waveguide electro-absorption modulator," J. Lightwave Technol. **34**, 419 (2016).
[11]D. J. Thomson, F. Y. Gardes, J. M. Fedeli, S. Zlatanovic, Y. Hu, B. P. P. Kuo, E. Myslivets, N. Alic, S. Radic, G. Z. Mashanovich *et al.*, "50-Gb/s silicon optical modulator," IEEE Photonics Technol. Lett. **24**, 234 (2012).
[12]T. Baba, S. Akiyama, M. Imai, N. Hirayama, H. Takahashi, Y. Noguchi, T. Horikawa, and T. Usuki, "50-Gb/s ring-resonator-based silicon modulator," Opt. Express **21**, 11869 (2013).
[13]E. Timurdogan, C. M. Sorace-Agaskar, J. Sun, E. Shah Hosseini, A. Biberman, and M. R. Watts, "An ultralow power athermal silicon modulator," Nat. Commun. **5**, 4008 (2014).
[14]Q. Xu, B. Schmidt, S. Pradhan, and M. Lipson, "Micrometre-scale silicon electro-optic modulator," Nature **435**, 325 (2005).
[15]Q. Xu, S. Manipatruni, B. Schmidt, J. Shakya, and M. Lipson, "12.5 Gbit/s silicon micro-ring silicon modulators," in *2007 Conference on Lasers and Electro-Optics, CLEO* (2007), Vol. 15, p. 430.
[16]M. Pantouvaki, P. Verheyen, J. De Coster, G. Lepage, P. Absil, and J. Van Campenhout "56Gb/s ring modulator on a 300 mm silicon photonics platform," in *2015 European Conference on Optical Communication (ECOC)* (2015), Vol. 4.
[17]L. Yang, R. Ji, L. Zhang, J. Ding, and Q. Xu, "On-chip CMOS-compatible optical signal processor," Opt. Express **20**, 13560 (2012).
[18]Z. Ying, Z. Wang, S. Dhar, Z. Zhao, D. Z. Pan, and R. T. Chen, "On-chip microring resonator based electro-optic full adder for optical computing," in *CLEO* (2017), pp. 4–5.
[19]Z. Zhao, Z. Wang, Z. Ying, S. Dhar, R. T. Chen, and D. Z. Pan, "Optical computing on silicon-on-insulator-based photonic integrated circuits," in *IEEE International Conference on ASIC* (2017), pp. 472–475.
[20]Z. Ying, Z. Wang, Z. Zhao, S. Dhar, D. Z. Pan, R. Soref, and R. T. Chen, "Silicon microdisk-based full adders for optical computing," Opt. Lett. **43**, 983 (2018).
[21]M. R. Watts, D. C. Trotter, R. W. Young, and A. L. Lentine, "Vertical junction silicon microdisk modulators and switches," Opt. Express **19**, 21989 (2011).
[22]T. Barwicz, H. Byun, F. Gan, C. W. Holzwarth, M. A. Popovic, P. T. Rakich, M. R. Watts, E. P. Ippen, F. X. Kärtner, H. I. Smith *et al.*, "Silicon photonics for compact, energy-efficient interconnects," J. Opt. Networking **6**, 63 (2007).
[23]J. Komma, C. Schwarz, G. Hofmann, D. Heinert, and R. Nawrodt, "Thermo-optic coefficient of silicon at 1550 nm and cryogenic temperatures," Appl. Phys. Lett. **101**, 41905 (2012).
[24]J. H. Choi, L. Wang, H. Bi, and R. T. Chen, "Effects of thermal-via structures on thin-film VCSELs for fully embedded board-level optical interconnection system," IEEE J. Sel. Top. Quantum Electron. **12**, 1060 (2006).
[25]L. G. L. Gu, W. J. W. Jiang, X. C. X. Chen, and R. T. C. R. T. Chen, "Thermooptically tuned photonic crystal waveguide silicon-on-insulator Mach–Zehnder interferometers," IEEE Photonics Technol. Lett. **19**, 342 (2007).
[26]X. Zhang, S. Chakravarty, C. J. Chung, Z. Pan, H. Yan, and R. T. Chen, "Ultra-compact and wide-spectrum-range thermo-optic switch based on silicon coupled photonic crystal microcavities," Appl. Phys. Lett. **107**, 221104 (2015).
[27]D. Kwong, A. Hosseini, Y. Zhang, and R. T. Chen, "1×12 Unequally spaced waveguide array for actively tuned optical phased array on a silicon nanomembrane," Appl. Phys. Lett. **99**, 051104 (2011).
[28]P. Dong, S. Liao, H. Liang, W. Qian, X. Wang, R. Shafiiha, D. Feng, G. Li, X. Zheng, A. V. Krishnamoorthy *et al.*, "High-speed and compact silicon modulator based on a racetrack resonator with a 1 V drive voltage," Opt. Lett. **35**, 3246 (2010).